Combined Signal Averaging and Electrocardiographic Imaging Method to Non-Invasively Identify Atrial and Ventricular Tachycardia Mechanisms

Corentin Dallet, Josselin Duchateau, Mélèze Hocini, Laura Bear, Marianna Meo, Frédéric Sacher, Michel Haïssaguerre, Rémi Dubois

IHU Liryc, Electrophysiology and Heart Modeling Institute, fondation Bordeaux Université, F-33600 Pessac-Bordeaux, France
Université de Bordeaux, CRCTB, U1045, F-33000 Bordeaux, France
INSERM, CRCTB U1045, F-33000 Bordeaux, France
Bordeaux University Hospital (CHU), Cardiac Electrophysiology and Cardiac Stimulation Team, F-33600 Pessac, France

Abstract

Current clinical electrocardiographic imaging (ECGi) aims to reconstruct epicardial signals using a single selected beat. However, minor sources of error that can be present on a beat-to-beat basis may affect the result, complicating arrhythmia mechanism identification and thus diagnosis and treatment. In this study, we applied signal averaging (SA) to ECGi on atrial and ventricular tachycardia diagnosis compared to a single beat approach. For that, a multi-lead SA algorithm was applied to QRS-complexes or atrial activity to obtain a robust template. Datasets came from patients with confirmed tachycardia obtained by invasive diagnosis. The non-invasive diagnosis was compared to the invasive with activation time maps and other clinical features in order to evaluate the contribution of SA versus the single beat approach (SB). The outcomes indicate that signal averaging improves the quality of non-invasive diagnosis for tachycardia reducing the diagnosis variability and the cycle length error (from 28% with SB to 13% with SA).

1. Introduction

Ventricular (VT) and atrial tachycardias (AT) are some of the most common clinical cardiac tachyarrhythmias. They are characterized by an abnormal and fast muscular activity and an organized electrical activity resulting from a change of electrical propagation. There are two dominate mechanisms for both tachycardias [1] [2]: reentry and focal activity. While methods already exist that use a catheter to provide sequential mapping and identify the underlying mechanism, these methods are invasive and time-consuming. Sometimes the arrhythmia cannot be induced during the procedure, and often the arrhythmia is not hemodynamically tolerated. Non-invasive electrocardiographic imaging [3] (ECGi) was developed to overcome some of these hurdles.

ECGi is used in clinical cardiology by computing the non-invasive reconstruction on a single user-selected heartbeat [4]. Nevertheless, due to the ill-posed nature of the inverse problem, the reconstruction is susceptible to sources of error, such as the electrode locations, far-field activity, signal amplitudes, and even the minor sources of error that are present in the single beat approach (SB): patient movements modifying waveform body surface electrocardiograms (ECGs) or surrounding noise hiding low amplitude signals. To reduce these errors, signal averaging (SA) methods have been developed and evaluated for arrhythmia diagnosis [5] but not for ECGi.

In this study, we evaluate the use of a multi-lead signal averaging algorithm (MLSA) combined to ECGi on non-invasive AT and VT diagnosis compared to the standard SB approach.

2. Multi-lead signal averaging algorithm

To evaluate the contribution of SA on ECGi compared to SB, a MLSA algorithm was developed. Initially designed for AT, it was based on the monomorphism of the P-wave resulting from AT (named f-wave) for both main mechanisms [2]. Hence, this method was also designed for monomorphic VT. The proposed SA algorithm consists in:

1) Removing QRS-complexes on each ECG to enhance atrial activity, only applied in case of AT
2) Selecting beats from the Pearson's correlation coefficient (CC) for the waveform analysis and the root-mean-square error (rMSE) for the amplitude analysis
3) Computing the average of the selected beats to get a robust complex for each lead

The aim of step 2 is to select the most representative beats pursuing the following process: i) the beats are located and ii) selected, or rejected, from the waveform and amplitude analysis. This process is performed on a reference ECG signal, named $\overline{ecg_{ref}}$. It is computed applying, firstly, a reduced-rank principal component analysis (PCA) on the ECGs set to get, at the most, 95% of the global information [6] and, secondly, a spatial averaging on the PCA-filtered ECGs. Then, after having located the beats with the cross-correlation between a manually chosen beat on $\overline{ecg_{ref}}$ and $\overline{ecg_{ref}}$, a selection is done between the identified beats. For that, a CC and a rMSE matrices are computed for all the detected beats and only the most representative ones are preserved. At the end of step 2, theirs locations are known on $\overline{ecg_{ref}}$ and thus on all the leads (Figure 1):

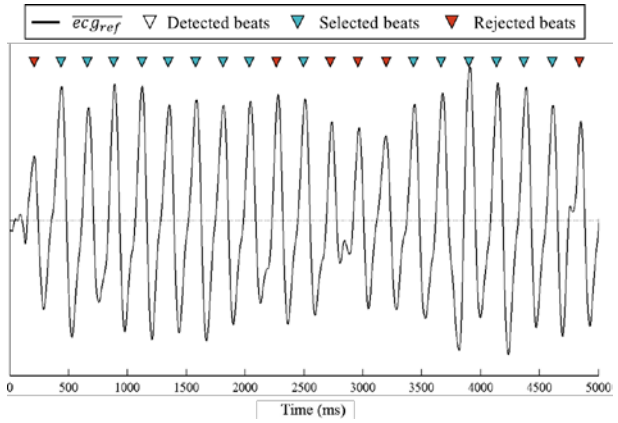

Figure 1. Example of $\overline{ecg_{ref}}$ with selected beats. In case of AT, a QT-interval is defined empirically from the ECGs (around 450 ms) to not select T-waves.

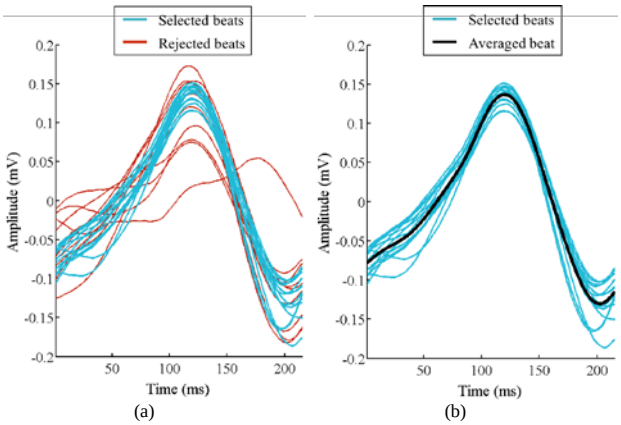

Figure 2. Example of a resulting averaged AT beat on a lead. (a) Rejected and selected f-waves after step 3. (b) Resulting averaged f-wave.

Finally, during step 3, from the locations got at step 2 on (ecg_ref), an average beat is computed on each lead (Figure 2).

3. Validation and comparison

3.1. Database

The database comes from patients with NaVX and/or CARTO system confirmed diagnosis acquired at Hôpital Haut-Lévêque. It includes 4 patients with monomorphic VTs; 8 post atrial fibrillation ATs in 6 patients (with n=3 roof-dependent macro-reentries, n=2 cavo-tricuspid isthmus dependent (CTI-dependent) flutters, n=2 peri-mitral flutters and n=1 roof foci [2]). For each pathology, geometric information of the patient was acquired with computed tomography and body surface potentials were recorded with a 252-electrode vest (CardioInsight). Epicardial unipolar single beat electrograms (EGMs) were reconstructed using the method of fundamental solutions [7].

3.2. Comparison features

To validate the proposed MLSA method and evaluate its contribution compared to SB, each selected beat (Section 2) was used to reconstruct a single beat EGM, simulating the current clinical process of ECGi with SB. Then, activation time maps, that allow identification of the underlying mechanism [2], were computed from the reconstructed single beat EGMs using [8]. From these maps, two outcomes are extracted i) the ratio of correct to incorrect non-invasive diagnosis, from the invasive, showing the variability of SB analysis and ii) the overall number of patients with the correct non-invasive diagnosis when compared to the invasive for SB and MLSA analysis. For SB analysis, the diagnosis for each patient was defined from the most occurring activation time map ("winner takes all" approach).

For ATs, the cycle length was estimated from the previous maps as well as the reconstructed propagation in the coronary sinus, one of the clinical features to identify the propagation in the left atrium [2]. These features were compared to the invasive recordings. A student's t-test was used to determine differences between MLSA and SB data. Statistical significance was accepted for $p < 0.05$

4. Results

Table 1 displays the variability of the non-invasive diagnosis using SB on all the selected beats. Table 2 lists the number of correctly diagnosed tachycardia using, on the one hand, the proposed MLSA and, on the other hand, SB according to the "winner takes all" criterion (Section 3).

Table 1. Overall variability of the non-invasive diagnosis using

SB on the 4 studied VTs and the 8 studied ATs.

	Nb. of selected beats with correct diagnosis	Percentage of correct diagnosis
VT (n=4)	117 on 136 selected	86.0 %
AT (n=8)	61 on 154 selected	39.6 %

Table 2. Patient non-invasive diagnosis validation using MLSA *versus* SB for the 4 studied VTs and the 8 studied ATs.

	SB	MLSA
VT (n=4)	4/4	4/4
AT (n=8)	1/8	8/8

The two following figures show examples of non-invasive activation time maps obtained using the proposed MLSA. In Figure 3-c, a crowding of isochrones on the posterior face gives the impression of a slow conduction area and therefore scar:

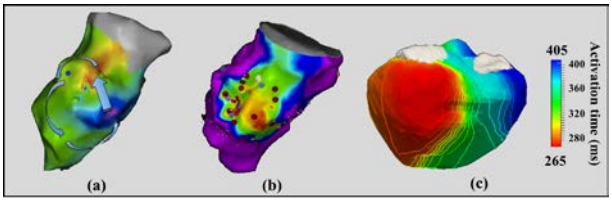

Figure 3. Patient with isthmus dependent monomorphic VT (adapted from [9]). (a) Invasive activation map. (b) Invasive voltage map with low voltage in red and high in purple. (c) Non-invasive activation time map (10ms step isochrones).

Figure 4 shows an activation initiated and terminated on the roof of the left atrium, area bounded by the pulmonary veins, and rotated around it, characteristics of a macro-reentrant AT from the roof:

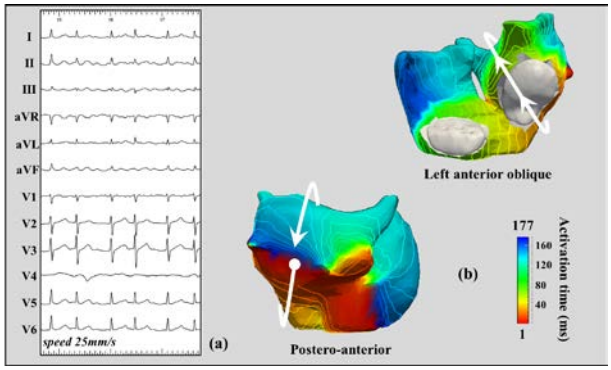

Figure 4. Patient with macro reentrant AT from the roof. (a) Twelve leads ECG. (b) Non-invasive activation time map (10ms step isochrones).

From these activation time maps, the cycle lengths were estimated for AT. Figure 5 displays the results in terms of cycle length with the absolute and relative AT cycle length error.

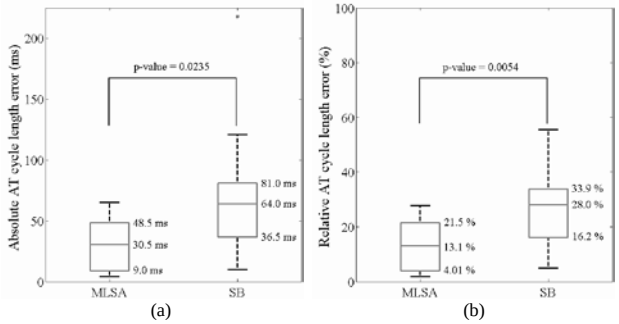

Figure 5. Comparison of AT cycle length between MLSA and SB. (a) Absolute cycle length error. (b) Relative cycle length error.

For both MLSA and SB, coronary sinus propagation was correctly reconstructed for 6 AT cases of 8 as illustrated in Figure 6 and Figure 7:

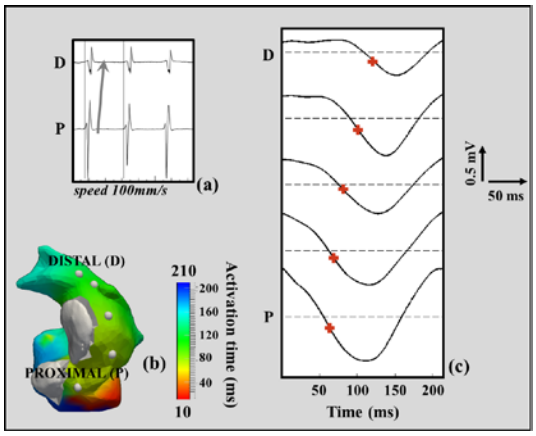

Figure 6. Coronary sinus propagation in a patient with CTI-dependent flutter. (a) Invasively recorded signals (b) Selected node locations. (c) Non-invasively reconstructed signals.

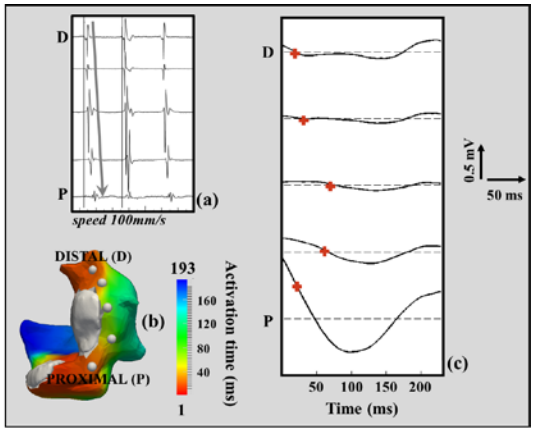

Figure 7. Coronary sinus propagation in a patient with peri-mitral flutter. (a) Invasively recorded signals (b) Selected node locations. (c) Non-invasively reconstructed signals.

Figure 6 shows a patient in which the reconstructed and the recorded coronary sinus propagation were the same, *i.e.* from proximal to distal. In contrast, Figure 7 presents a

case where recorded coronary sinus propagation spread from distal to proximal, whereas the reconstructed propagation was less obvious to identify.

5. Discussion and conclusions

Globally, SA improves the quality of the non-invasive reconstruction compared to SB. Nevertheless, its contribution differs between AT and VT.

Regarding the validation of the diagnosis (Tables 1 & 2), the proposed MLSA reproduces the correct diagnosis for all the studied patients whereas, on a SB basis, the correct diagnosis was given for 1 patient with AT (with less than 50% of the selected f-waves reproducing it) and all VT patients (with 86% of the selected QRS-complexes). Hence, SA reduces the variability and improves the efficacy of the non-invasive diagnosis with ECGi. These differences could come, first, from a higher signal-to-noise ratio on f-waves. Indeed, the low amplitudes, around 0.2 mV, make them more susceptible to noise compared to QRS-complexes (amplitude is around 1 mV). Secondly, the studied VT are more stable than the studied AT, reducing the effects of MLSA on the reconstruction.

Despite this, coronary sinus propagation was the same for both MLSA and SB: for two cases, the reconstructed propagation was incorrect. This may be due to misplacement of the activation time marker placement (Figure 7) as a result of the low amplitude of the signals. Suboptimal f-waves selection could lead to this poor reconstruction without affecting the reconstruction of the underlying mechanism. Indeed, to clearly identify the propagation in the left atrium, more features are needed such as the propagation near the esophagus [2]. Therefore, as ECGi aims to provide a global overview of the underlying mechanism, this local feature cannot be used to validate or invalidate the reconstruction. Nevertheless, the propagation is correctly identified for 6 pathologies of 8 (Figure 6).

Regarding the cycle length of the AT, ECGi has a known limitation of reducing activation time dispersion [10]. That is, the torso volume smooths high spatial frequencies of source distributions, leading to poor reconstruction at the onset and the offset of the activation [11]. Normally, the shorter activation duration leads to poor estimation of conduction velocity. With this improvement on the temporal estimation with SA, local conduction velocity estimation using ECGi may also be improved [12].

In summary, SA improves the quality of non-invasive diagnosis for tachycardia, reducing some limitations of ECGi. This improvement could complete the non-invasive diagnosis with other features such as the conduction velocity.

This work was supported by Grant ANR-10-IAHU-04.

References

[1] Kléber AG, Rudy Y. Basic mechanisms of cardiac impulse propagation and associated arrhythmias. Physiol Rev. 2004;84(2):431–88.

[2] Saoudi N, Cosion F, Waldo A, Chen SA, Iesaka Y, Lesh M, et al. A classification of atrial flutter and regular atrial tachycardia according to electrophysiological mechanisms and anatomical bases. A Statement from a Joint Expert Group from the Working Group of Arrhythmias of the European Society of Cardiology and the. Eur Heart J. 2001;22(14):1162–82.

[3] Rudy Y, Burnes JE. Noninvasive electrocardiographic imaging. Ann Noninvasive Electrocardiol. 1999;4(3):340–59.

[4] Ramanathan C, Ghanem RN, Jia P, Ryu K, Rudy Y. Noninvasive electrocardiographic imaging for cardiac electrophysiology and arrhythmia. Nat Med. 2004;10(4):422–8.

[5] Holmqvist F, Platonov PG, Havmöller R, Carlson J. Signal-averaged P wave analysis for delineation of interatrial conduction - further validation of the method. BMC Cardiovasc Disord. 2007;7(1):29.

[6] Meo M. Spatio-temporal characterization of the surface electrocardiogram for catheter ablation outcome prediction in persistent atrial fibrillation. Université de Nice Sophia Antipolis; 2014.

[7] Wang Y, Rudy Y. Application of the method of fundamental solutions to potential-based inverse electrocardiography. Ann Biomed Eng. 2006;34(8):1272–88.

[8] Dubois R, Labarthe S, Coudière Y, Hocini M, Haïssaguerre M. Global and directional activation maps for cardiac mapping in electrophysiology. Comput Cardiol. 2012;39:349–52.

[9] Berte B. Characterization by Imaging and High-density Electrophysiology of Ventricular. Université de Bordeaux; 2015.

[10] Han C, Liu Z, Zhang X, Pogwizd SM, He B. Noninvasive three-dimensional cardiac activation imaging from body surface potential maps: A computational and experimental study on a rabbit model. IEEE Trans Med Im. 2008;27(11):1622–30.

[11] Schneider F, Dossel O, Muller M. Filtering characteristics of the human body and reconstruction limits in the inverse problem of electrocardiography. Comput Cardiol. 1998;25:689–92.

[12] Dallet C, Bear L, Duchateau J, Potse M, Zemzemi N, Meillet V, et al. Local Conduction Velocity Mapping for Electrocardiographic Imaging. Comput Cardiol. 2015;225–8.

Address for correspondence.
Corentin Dallet, corentin.dallet@ihu-liryc.fr
IHU LIRYC, Avenue du Haut-Lévèque, Pessac France